Journal of Glaciology, Vol. 25, No. 93, 1980

SNOW-AVALANCHE IMPACT ON STRUCTURES

By THEODORE E. LANG *and* ROBERT L. BROWN

(Department of Civil Engineering and Engineering Mechanics, Montana State University, Bozeman, Montana 59717, U.S.A.)

ABSTRACT. Two-dimensional hydrodynamic equations for laminar, viscous flow, and admitting a frictional slip-plane lower boundary are applied to the modeling of snow-avalanche impact on rigid wall structures. Predicted maximum pressures and pressures versus time are compared with published experimental results, and general correspondence is established. Impact pressure versus time is found to depend upon the shape of the avalanche leading edge, for which general information is lacking. Computer modeling of more complex structural configurations is feasible using the methodology reported.

RÉSUMÉ. *Impact des avalanches de neige sur des ouvrages.* On applique les équations hydrodynamiques à deux dimensions pour un écoulement laminaire, visqueux et admettant à son extrémité inférieure un plan de glissement à frottement pour une modélisation de l'impact d'une avalanche de neige sur des ouvrages à paroi rigide. Les pressions maximum prévues et les variations des pressions avec le temps sont comparées aux résultats expérimentaux publiés, et une correspondance générale est établie. On montre que la pression d'impact en fonction du temps dépend de la forme de la tête de l'avalanche pour laquelle on manque en général d'information. Une modélisation mathématique de configurations structurelles plus complexes est possible en utilisant la méthodologie rapportée.

ZUSAMMENFASSUNG. *Der Anprall von Schneelawinen auf Bauwerke.* Zur Modellierung des Anpralls von Schneelawinen auf starre Wände werden zweidimensionale hydrodynamische Gleichungen für laminares, viskoses Fliessen herangezogen, welche die Einführung einer Gleitfläche mit Reibung als unterer Begrenzung gestattet. Berechnete Maximaldrucke und zeitliche Druckabläufe werden mit veröffentlichten experimentellen Ergebnissen verglichen, wobei sich im allgemeinen Übereinstimmung zeigt. Es ergibt sich, dass der Anpralldruck zeitlich von der Form der Lawinenfront abhängt, über die allgemein zu wenig bekannt ist. Modellrechnungen für kompliziertere Bauwerksformen nach der geschilderten Methode erscheinen zweckmässig.

INTRODUCTION

Summarized is a new methodology for predicting forces and pressures on structures caused by impact by snow avalanches. Snow flow and impact are represented in an iterative, finite-difference algorithm applied to two-dimensional Navier–Stokes equations of an incompressible Newtonian fluid. These equations, for laminar flow, are determined to represent the flow of the dense, core material of a snow avalanche, based upon viscosity estimates established for snow-avalanche run-out (Lang and others, 1979). These estimates result in predicted Reynolds numbers below 1 000, well within the laminar flow regime. The condition of incompressibility of the flow at impact is an approximation for snow that results in conservative estimates of forces in structural design evaluations. The general lack of detailed information on flow properties of snow, such as distribution of mass with depth, air entrapment effects, material compressibility properties, and others, makes it sensible only to model the general dynamic response. The close correspondence between computer model prediction and corresponding data by Salm (1964) reported by Pedersen and others (1979), provides evidence for the adequacy of the computer code to represent avalanche impact.

The advance of the fluid as time proceeds through the finite-difference grid of the flow domain is carried out by iterative refinement of the momentum and mass distributions consistent with the governing equations. The original report of a computer algorithm for two-dimensional flow in either a closed or free-surface domain was given by Hirt and others (1975). Modification of this general-purpose code to the specific modeling of avalanche flow (program AVALNCH) has been reported by Lang and others (1979) and Lang and Martinelli (1979).

Basic contributions to the understanding of the snow-impact problem date back to the work by Voellmy (1955), in which he evaluates evidence from several avalanches in Austria. He concludes that pressures in the range of 100 to 200 kN/m² are necessary to account for the damage noted. For calculation of impact pressure, Voellmy proposes a version of the dynamic pressure equation with pressure proportional to the square of the flow velocity (or to the kinetic energy).

Furukawa (1957) reported the results of releasing snow blocks to slide down a slope and impact against a wall. Average measured pressure at impact correlated to other parameters by the equation

$$p = 35(1.35v^2\rho^{1.5}/g)^{0.45}\ \mathrm{kN/m^2},$$

applicable in the range of density $150\ \mathrm{kg/m^3} < \rho < 550\ \mathrm{kg/m^3}$, impact velocity $5\ \mathrm{m/s} < v < 20\ \mathrm{m/s}$, and $g = 9.8\ \mathrm{m/s^2}$. The time constant of the recording oscillograph of these experiments was 0.01 s, so that rapid variations of the loading were smoothed. Pressures computed by Furukawa's equation fall into the same range as those reported by Voellmy.

Saito and others (1963) reported results of experiments made on various avalanche control structures. For posts set up in avalanche paths, maximum measured impact pressure was 300 kN/m² and ranged downward to an average for all tests around 200 kN/m².

A year later, Salm (1964) reported results similar to those of Furukawa, except that the force-recording equipment had a shorter time constant, so that millisecond duration pulses were detected. For snow blocks impacting at velocities of 11 to 13 m/s, average pressures were obtained in the range 150 to 200 kN/m² for impact onto an elastically soft wall. Maximum pressures of load pulses of several milliseconds duration were found to be 2 to 5 times larger than these average pressures.

Perhaps the most complete set of data on avalanche impact was reported by Schaerer (1973) based upon a number of avalanche measurements made at Rogers Pass, Canada. Pressure gages mounted on posts in avalanche paths were used to monitor average impact pressure. Measurements were made also of depth of flow, nominal snow density of the debris, and average avalanche speed. Using a dynamic pressure equation, Schaerer compared computed and measured pressures. Averaged pressures ranged from 30 to 260 kN/m² for avalanche speeds from 15 to 53 m/s and flow depths between 1.5 m and 1.8 m as evidenced from snow deposits on trees and side walls of the flow channels.

Additional evidence was reported by Mears (1975) based upon analysis of damaged trees in the path of an avalanche in Colorado. For flow speeds of 18 m/s, loading was estimated at 80 to 100 kN/m² for a flow height of 1.1 m and snow density of 300 kg/m³.

These cited results tend to establish average impact pressures up to 300 kN/m² for flow velocities up to, say, 50 m/s, although incomplete data reporting tends to preclude any conclusive statements about the range.

Results of a different type were reported by Shimizu and others (1974) based upon measurements of three avalanches in Kurobe canyon, Japan. Indications from the discussion of this work are that the avalanches are high speed, however no information is presented on actual velocities. Pressures were reported to vary from 320 to 1 340 kN/m² depending upon the type of recording system. A maximum pressure of 2 100 kN/m² was mentioned without detailed explanation. Lacking information on the response of the recording system and the flow velocities, it is possible to attribute these high pressures either to high velocity of impact, or to reporting of maximum pressures of load pulses, as is done by Salm (1964) and Schaerer (1973), rather than of pressure averaged over 10 to 100 ms.

Having an indication of the nature of the force history of typical avalanche impact, we investigate the possibility of computer simulation of the phenomenon. Should the computer simulation prove accurate, a basis would exist for development of design criteria by means other than accumulation of physical data from random physical events.

Governing equations and flow parameters

In considering the flow of a snow avalanche, we make a distinction between the flow characteristics of a possible airborne component of the flow, and the flow of the denser or core component. Our consideration is directed to the core component, which has a typical velocity range of 20 to 50 m/s. The core component, because of its large internal viscosity, is in laminar flow with internal circulation. Numerical analysis of the impact is with respect to a typical cross-section of the flow, so that two-dimensional forms of the governing Navier–Stokes equations are used, namely

$$\frac{\mathrm{d}u}{\mathrm{d}t} = X - \frac{1}{\rho}\frac{\partial p}{\partial x} + \nu\left(\frac{\partial^2 u}{\partial x^2} + \frac{\partial^2 u}{\partial y^2}\right), \tag{1}$$

$$\frac{\mathrm{d}v}{\mathrm{d}t} = Y - \frac{1}{\rho}\frac{\partial p}{\partial y} + \nu\left(\frac{\partial^2 v}{\partial x^2} + \frac{\partial^2 v}{\partial y^2}\right), \tag{2}$$

where u, v are velocity components; X, Y are body-force components, ρ is fluid density; ν is kinematic viscosity, and p is the pressure. Additionally,

$$\frac{\mathrm{d}}{\mathrm{d}t} = \frac{\partial}{\partial t} + u\frac{\partial}{\partial x} + v\frac{\partial}{\partial y}.$$

These equations are based upon the assumption of fluid incompressibility, recognized as a conservative approximation for flowing snow during impact. Material incompressibility is expressed through the two-dimensional divergence criterion that

$$\frac{\partial u}{\partial x} + \frac{\partial v}{\partial y} = 0. \tag{3}$$

Stresses acting upon a fluid element are defined by

$$\left.\begin{aligned} \tau_{xx} &= -p + 2\nu\rho\frac{\partial u}{\partial x}, \\ \tau_{yy} &= -p + 2\nu\rho\frac{\partial v}{\partial y}, \\ \tau_{xy} &= \nu\rho\left(\frac{\partial v}{\partial x} + \frac{\partial u}{\partial y}\right). \end{aligned}\right\} \tag{4}$$

Equations (1) through (4), expressed in finite-difference form, are used to simulate the avalanche flow by step-wise time incrementation using a computer algorithm reported by Hirt and others (1975). The finite-difference grid that represents the flow domain plus a layer region with a one-cell thickness is shown in Figure 1. Slope angle is ϕ and initial angle of the leading edge of the avalanche is ψ_L. Surface friction is defined by specifying the x component of velocity in the lower boundary cell u_1 as a fraction of the velocity in the adjacent flow-domain cell u_2 by the equation

$$u_1 = u_2(1 - 2f), \tag{5}$$

where f is the surface friction coefficient. If $f = 0$ then $u_1 = u_2$ and the boundary is slip-free. If $f = 1$ then $u_1 = -u_2$ and velocity at the interface between the cells is zero, which is a no-slip condition. For avalanche flow $0.35 \leqslant f \leqslant 0.6$ is the range that typically represents most cases, and for purposes of study of impact $f = 0.5$ is used. A second basic parameter in the definition of avalanche flow is the internal kinematic viscosity ν. Based upon a number of empirical case studies of avalanche flows, a nominal value of $\nu = 0.5$ m²/s is used for the impact modeling.

https://doi.org/10.3189/S002214300001529X Published online by Cambridge University Press

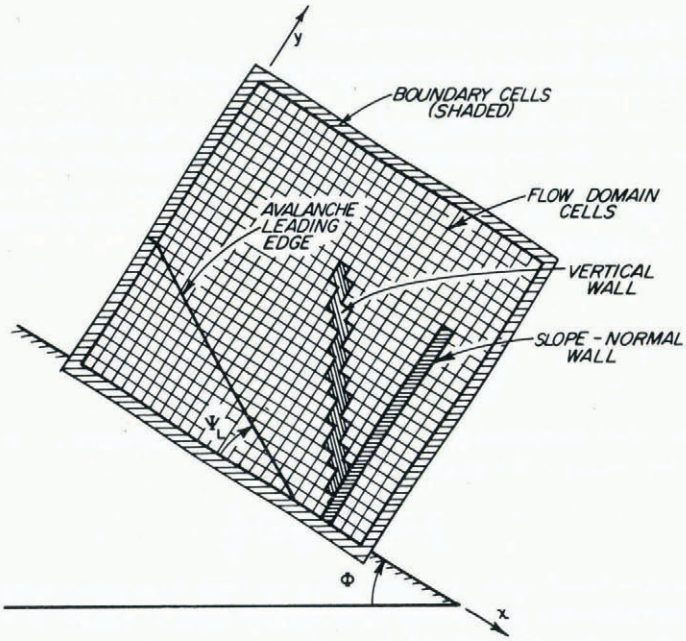

Fig. 1. Arrangement of finite-difference grid, avalanche leading edge, and slope-normal (or vertical) impact wall.

Two other boundary conditions complete the specification of the problem. An additional condition at the lower boundary, independent from the value of f, is that velocity normal to the surface is zero, which represents the case of a rigid, stationary surface. A continuity inflow condition is imposed at the up-hill boundary ($x = 0$), which maintains flow height and velocities in the boundary cells that are initially specified.

Impact upon a slope-normal wall

Much of the experimental data from load-cell measurements is taken from test rigs in which the sensing elements are arrayed in a line normal to the slope surface. Thus, direct comparison of experimental data and computer simulation data is possible using a slope-normal wall (Fig. 1). Additionally, avalanche defense structures are usually constructed with a slope-normal up-hill surface, thereby making this geometry particularly relevant. The leading edge of the avalanche is initially defined by the angle ψ_L, and material in all cells to the left of the leading edge are given an initial slope-parallel speed in the range of equilibrium speed for avalanche flow on a slope of angle ϕ. This initial assumption is not correct, but in the first cycle of computations of establishing mass continuity, the velocity and pressure values in each cell are adjusted to meet specified compatibility requirements. This results in a change of the shape of the leading-edge profile from a straight line. If the initial velocity estimate is accurate, then the compatibility correction is small, and what ensues is a flow in which the leading-edge geometry changes, but the nominal speed of the entire mass does not systematically change with advance of the flow. In all cases, computer runs were made with different initial velocity estimates until the flow showed the persistence in velocity as described above.

The problem set up is shown in Figure 1. The total flow domain is modeled by 30 cells along the slope and 30 cells normal to the slope. All cells are square of dimension 0.05 m on a side. The slope-normal wall is placed in cell No. 24, and the leading edge of the avalanche

terminates in cell No. 21 at the start of the flow. The wall is simulated by zeroing velocity components in the appropriate cells for all time and in all calculations (this assumption is equivalent to setting $f = 0.5$, the same condition as on the lower boundary of the flow). Output from the program consists of a listing of pressure per unit density, velocity components, and flow height for each cell at any specified time during impact. Normal and shear forces, and bending moment at the base of the wall are computed at each time increment of the computations. All force computations are per unit density of material.

For purposes of illustration, we summarize a typical impact condition. We set the slope angle at $\phi = 30°$, the leading-edge angle at $\psi_L = 30°$, nominal slope-parallel flow velocity at $U_0 = 20$ m/s, and viscosity and friction at $\nu = f = 0.5$. One type of result is the change in shape of the leading edge of the avalanche as the flow progresses (Fig. 2). At the instant of impact, the leading elements of the flow have changed to an impact angle $\psi_I = 76°$. Following initial contact, the avalanche front piles against the wall with the profile sequence depicted in Figure 2. Although snow height on the wall is accurately resolved after impact by interpolation, the shape of the leading edge is an approximation based upon height estimates every 0.05 m from the wall. Thus, impact angle ψ_I is also an estimated quantity (Fig. 2). Maximum pressure and maximum normal force on the wall occur when the flow surface is approximately parallel to the slope at $T = 8.3$ ms.

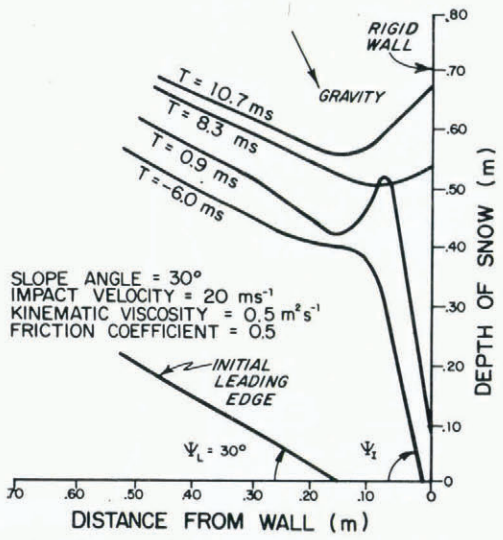

Fig. 2. Distribution of snow up-slope from a rigid slope-normal wall at several times T measured from the time of impact.

The distribution of pressure along the wall for several time intervals after initial impact, corresponding to different snow profiles of Figure 2, is shown in Figure 3. The pressure distribution at $T = 8.3$ ms is 0.1 ms off the time at which pressure is maximum at $(p/\rho)_{max} = 2\,500$ m²/s². The time histories of the normal and shear forces and base moment are shown in Figure 4. It is seen that the forces peak at approximately 8.3 ms into the impact, and persist for approximately 1.5 ms.

By varying the initial leading edge angle ψ_L, different impact angles and load histories are obtained. Using a reference snow density of $\rho = 300$ kg/m³ actual maximum and average pressures can be calculated. These results are summarized in Table I. One significant result is the large difference between average and maximum pressure of an order-of-magnitude. By averaging pressure over 100 ms, which corresponds to the time constant of most measuring

https://doi.org/10.3189/S002214300001529X Published online by Cambridge University Press

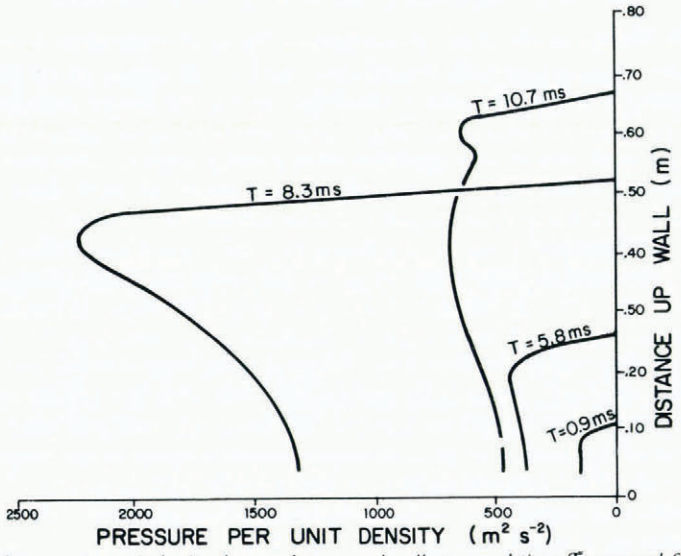

Fig. 3. Distribution of pressure per unit density along a slope-normal wall at several times T measured from the time of impact.

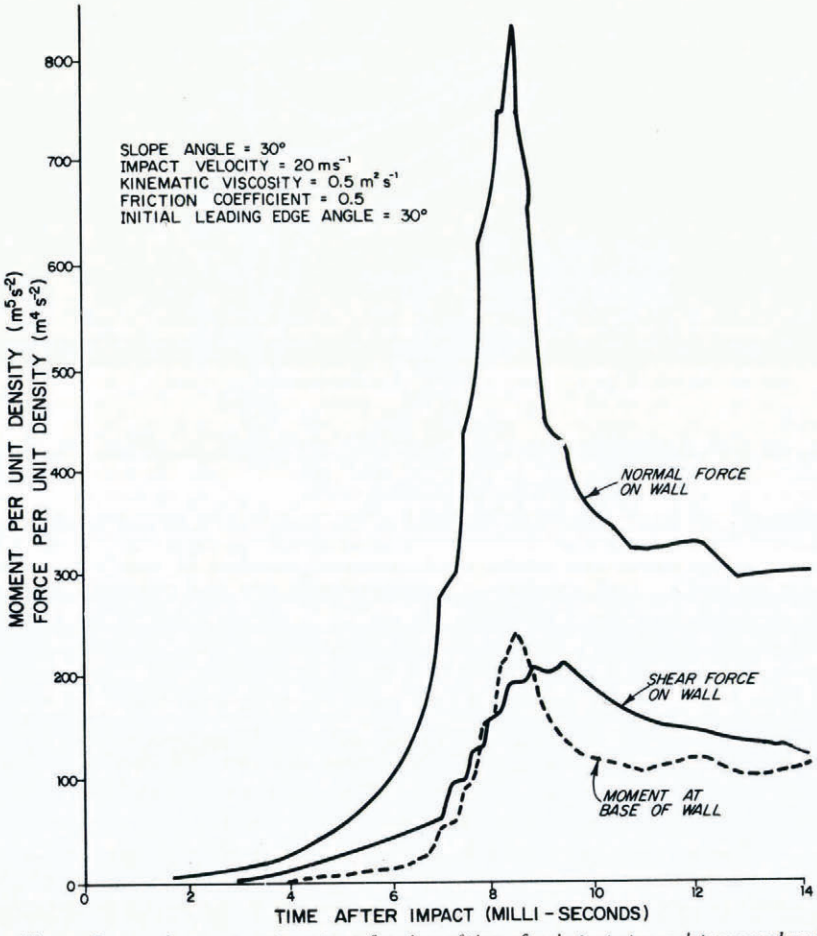

Fig. 4. Force and moment components as functions of time after impact upon a slope-normal wall.

https://doi.org/10.3189/S002214300001529X Published online by Cambridge University Press

TABLE I. VARIATION IN IMPACT ANGLE, PRESSURE, AND WALL FORCES AS A FUNCTION OF INITIAL LEADING-EDGE ANGLE FOR A SLOPE-NORMAL WALL IMPACTED AT 20 m/s

Initial leading-edge angle ψ_L deg	*Estimated impact angle* ψ_I deg	*Maximum pressure** kN/m²	*Average pressure†* kN/m²	*Snow height on wall at maximum pressure* m	*Maximum normal force per unit density* m⁴/s²	*Maximum shear force per unit density* m⁴/s²	*Maximum bending moment per unit density* m⁵/s²
30	76	76.5	9.3	0.53	830	200	240
45	80	144	13.9	0.55	1 750	320	500
60	81	205	18.4	0.63	2 800	500	1 000
75	86	266	25.0	0.95	5 800	1 300	3 600
80	88	297	26.0	1.25	7 200	1 600	5 000

* Based upon a snow density of 300 kg/m³. Note: no correlation between maximum pressure and maximum forces.

† Pressure averaged for 100 ms after impact.

equipment used to date, pressures in the range of reported values are obtained. A plot of maximum and average pressure as a function of estimated impact angle (Fig. 5) indicates an approximate linear variation between parameters.

By changing the angle of the ground surface, avalanches with different equilibrium velocities can be modeled. In doing this flow velocities of 7, 10, 15, and 30 m/s provide supplemental data to the reported case of 20 m/s. Through this parameterization, we summarize the variation in maximum and average pressure versus nominal flow or impact speed

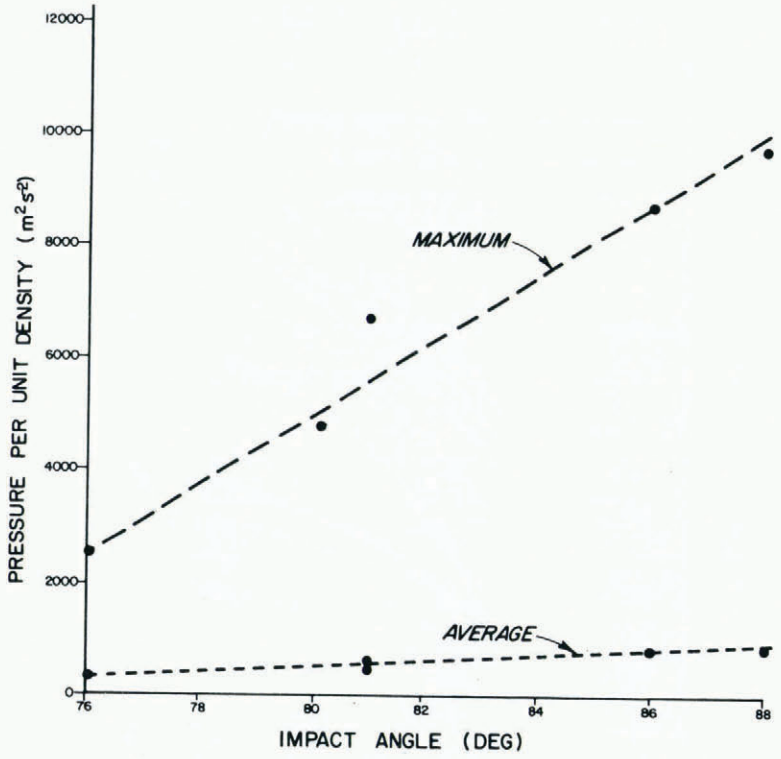

Fig. 5. Variation in maximum and average pressures with estimated leading-edge angle for impact at 20 m s⁻¹ onto a slope-normal wall.

https://doi.org/10.3189/S002214300001529X Published online by Cambridge University Press

in Figure 6. Results obtained for a flow speed of 7 m/s show no pressure peak, but rather a monotonic increase in pressure as the snow piles against the wall. By extrapolation of pressure to 90° in plots like Figure 5 for all cases, the pressure curves of Figure 6 indicated as limit pressure are obtained.

Impact upon a vertical wall

The case of a vertical wall is shown also in Figure 1. Apart from the stepwise geometry complicating calculation of wall forces and base moment, the evaluation procedure is the same as with the slope-normal wall.

In the case of the vertical wall, the angle between the wall and the up-slope ground surface is 60°. Using the same avalanche description as with the slope-normal wall, initial leading edge angles of 30°, 45°, 60°, and 75° increase to angles equal to or greater than 76° at impact. For these angles of the leading edge, in the case of a vertical wall the upper parts of the leading edge contact the wall prior to contact at the base. Thus, we can expect different pressure and force histories for the two geometries. Detailed variations of normal force, shear force, and base moment on the vertical wall for the case of a 30° initial leading edge (impact velocity of 20 m/s) avalanche are shown in Figure 7. No attempt is made to plot the pressure distribution of the snow surface at contact because of uncertainty as to the area of contact as a function of time. Rigorous determination of this information requires considerable grid refinement. Maximum pressures and average pressures over 100 ms duration of impact are tabulated in Table II. Although maximum pressures show a wide variation among the four cases, average pressure varies by only a factor of 1.6, whereas this factor is 2.8 for the corresponding slope-normal wall.

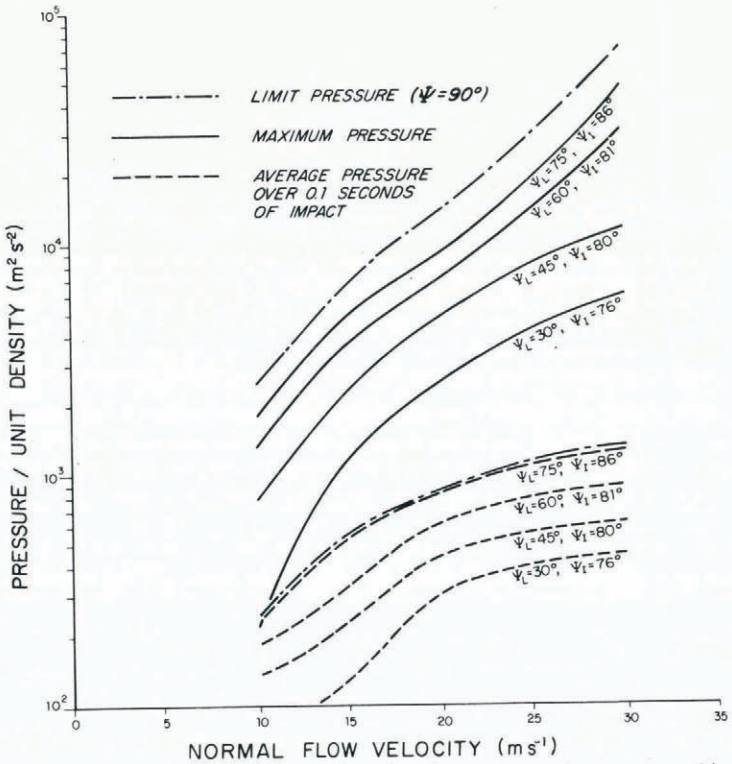

Fig. 6. Variation of pressure with normal flow velocity for different leading-edge angles on impact with a slope-normal wall.

https://doi.org/10.3189/S002214300001529X Published online by Cambridge University Press

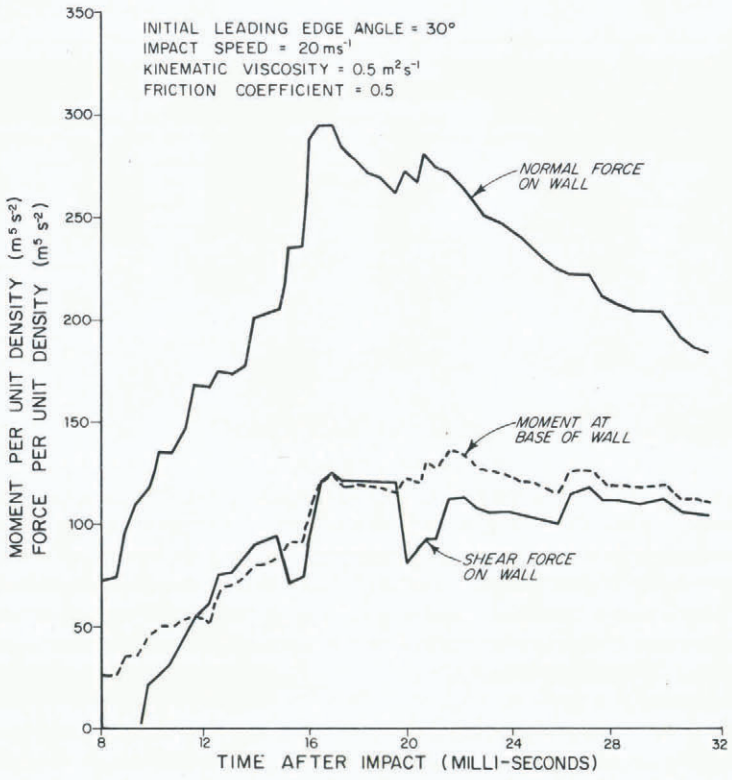

Fig. 7. Force and moment components as a function of time after impact upon a vertical wall.

TABLE II. VARIATION IN PRESSURE WITH INITIAL LEADING-EDGE ANGLE FOR THE VERTICAL WALL GEOMETRY AND AN IMPACT VELOCITY OF 20 m/s

Leading-edge angle deg	*Maximum pressure** kN/m²	*Average pressure over 100 ms duration* kN/m²
30	224	86
45	370	98
60	676	104
75	3 260	138

* Based upon a snow density of $\rho = 300$ kg/m³.

CONCLUSIONS FROM SLOPE-NORMAL AND VERTICAL WALL RESULTS

Although the computer solutions include calculations of forces and moments on the slope-normal and vertical walls, which is essential information for design, we consider pressure as the fundamental quantity for comparison of the two cases. The average and maximum pressures per unit density for the two cases are tabulated in Table III. For impact angles of 76°, 80°, and 81°, the slope-normal wall pressures are larger than corresponding vertical-wall pressures, with larger differences noted for maximum pressures than for average pressures. At an impact angle of 86°, the maximum pressure on a vertical wall jumps to a value larger

https://doi.org/10.3189/S002214300001529X Published online by Cambridge University Press

TABLE III. AVERAGE AND MAXIMUM PRESSURES GENERATED ON SLOPE-NORMAL AND VERTICAL WALLS AS A FUNCTION OF LEADING-EDGE IMPACT ANGLE AT AN IMPACT VELOCITY OF 20 m/s

	Slope-normal wall		*Vertical wall*	
Leading-edge impact angle deg	*Maximum pressure per unit density* m^2/s^2	*Average pressure* per unit density* m^2/s^2	*Maximum pressure per unit density* m^2/s^2	*Average pressure* per unit density* m^2/s^2
76	2 500	305	730	280
80	4 700	455	1 200	320
81	6 700	600	2 200	340
86	8 700	815	10 600	450
88	9 700	850	—	—

* Averaged over initial 100 ms of impact.

than the corresponding value for the slope-normal case. Not knowing the geometric configuration of the leading edge of the avalanche as it impacts the vertical wall, we can only hypothesize that the increased pressure is due to near-parallel contact between the snow surface and the wall at some point above the base of the wall at impact. The result of this is a generated pressure of 10 600 m^2/s^2 per unit density that peaks and subsides in less than a millisecond. This is followed by a pressure tail-off such that average pressure over 100 ms is comparable to that of the cases with other impact angles. This "wave-slapping" action, well recognized in water-wave phenomena, apparently can occur in avalanche impact also, and constitutes a limiting case in pressure generation.

The limiting pressures of Figure 6 are obtained by assuming avalanche impact onto a rigid wall. Any wall flexibility can be expected to decrease the limiting pressure. Additionally, compressibility of the snow itself should also tend to decrease pressure. Based upon the pressure peaking, which occurs in all cases of slope-normal wall impact, the question arises whether a pressure pulse of 1.0 to 2.0 ms duration can have significant effect on structures. Results of tests on small steel specimens (Newmark and Haltiwanger, 1962) show that stresses on the order of twice the yield stress, when applied rapidly, can cause material yielding and fracture within 1.0 ms. However, extrapolation of this result to, say, reinforcing steel is not apparent. Although stresses on structures may develop to values beyond yielding or fracture, strains necessary for the failure will not develop in structures because of the large inertia. Thus, for typical structures made of steel, concrete, or wood, it is unlikely that the millisecond-duration pulse will have a significant effect, and design should be based upon average pressure response.

From these results, we conclude that the specific shape of the leading edge of the avalanche at impact has a significant effect on the maximum pressure that is generated. A worst-case geometry has been evaluated from this computer study; however, the statistical probability of this occurrence is not known. To obtain supporting data from field observations, advanced avalanche-observation techniques must be developed which allow penetration of the usual snow–air cloud that accompanies all but the slowest-moving dry-snow avalanches. Alternate courses of action might be to base a computer model of steady-state snow flow upon improved definition of the flow parameters, or to set up columns of sensitive pressure transducers from which differential arrival times of actual avalanches could be detected.

Although physical data on snow-avalanche impact are sparce, qualitative comparison between our computer results and experimental results by Salm (1964) is useful. For impact against a slope-normal wall, the pressure peaks measured by Salm are two to five times greater than average pressures reported, and the pulses show durations on the order of 5 to 10 ms. Our results show maximum pressures to be as much as eleven times greater than average pressures and the pulses last 1 to 2 ms. Whereas the computer results are for impact onto a rigid wall,

the impact in Salm's experiments is against an elastic wall (elasticity information not reported). Physical reasoning predicts the spreading of the pulse and decrease in maximum pressure as the impact surface goes from rigid to elastic and so supports these qualitative observations.

The principal conclusion we derive from these computer studies is that program AVALNCH (Lang and others, 1979; Lang and Martinelli, 1979) has modeling capability for avalanche impact. Uncertainties as to leading-edge geometry prevent explicit prediction of the range of expected pressures; however, preliminary results show that upper limits on pressures can be established.

Acknowledgements

The authors wish to acknowledge the financial support provided by the U.S. Forest Service, Rocky Mountain Forest and Range Experiment Station, Fort Collins, Colorado, under cooperative agreement no. 16-778-CA, and the Department of Civil Engineering and Engineering Mechanics, Montana State University, Bozeman, Montana.

MS. received 27 February 1979 and in revised form 23 May 1979

REFERENCES

Furukawa, I. 1957. Yukikuzure no shōgekiryoku [Impact of avalanches]. *Seppyō*, Vol. 19, No. 5, p. 140–41.

Hirt, C. W., *and others*. 1975. *SOLA: a numerical solution algorithm for transient fluid flows, by C. W. Hirt, B. D. Nichols, and N. C. Romero*. Los Alamos, New Mexico, Los Alamos Scientific Laboratory. (Report No. LA 5852.)

Lang, T. E., *and* Martinelli, M., *jr*. 1979. Application of numerical transient fluid dynamics to snow avalanche flow. Pt. 2. Avalanche modeling and parameter error evaluation. *Journal of Glaciology*, Vol. 22, No. 86, p. 117–26.

Lang, T. E., *and others*. 1979. Application of numerical transient fluid dynamics to snow avalanche flow. Pt. 1. Development of computer program AVALNCH, by T. E. Lang, K. L. Dawson, and M. Martinelli, Jr. *Journal of Glaciology*, Vol. 22, No. 86, p. 107–15.

Mears, A. I. 1975. Dynamics of dense-snow avalanches interpreted from broken trees. *Geology*, Vol. 3, No. 9, p. 521–23.

Newmark, N. M., *and* Haltiwanger, J. D. 1962. *Air Force design manual. Principles and practices for design of hardened structures*. Kirtland Air Force Base, New Mexico, U.S. Air Force Special Weapons Center. (AFSWC-TDR-62-138.)

Pedersen, R. R., *and others*. 1979. Forces on structures impacted and enveloped by avalanches, by R. R. Pedersen, J. D. Dent, and T. E. Lang. *Journal of Glaciology*, Vol. 22, No. 88, p. 529–34.

Saito, S., *and others*. 1963. Study on avalanche preventive steel structures, by S. Saito [and 6 others]. *NKK Steel Note* (Tokyo), 1963, No. 3, p. 57–66.

Salm, B. 1964. Anlage zur Untersuchung dynamischer Wirkungen von bewegtem Schnee. *Zeitschrift für angewandte Mathematik und Physik*, Vol. 15, Fasc. 4, p. 357–75.

Schaerer, P. A. 1973. Observations of avalanche impact pressures. *U.S. Dept. of Agriculture. Forest Service. General Technical Report* RM-3, p. 51–54.

Shimizu, H., *and others*. 1974. Kurobe-kyōkoku kōsoku-nadare no kenkyū. 3 [Study on high-speed avalanches of Kurobe Canyon. 3]. [By] H. Shimizu [and 5 others]. *Teion-kagaku: Low Temperature Science*, Ser. A, [No.] 32, p. 113–27.

Voellmy, A. 1955. Über die Zerstörungskraft von Lawinen. *Schweizerische Bauzeitung*, Jahrg. 73, Ht. 12, p. 159–62; Ht. 15, p. 212–17; Ht. 17, p. 246–49; Ht. 19, p. 280–85. [English translation: On the destructive force of avalanches. *U.S. Dept. of Agriculture. Forest Service. Alta Avalanche Study Center Translation* No. 2, 1964.]